Original Research Paper

Volume-8 | Issue-3 | March-2018 | PRINT ISSN No 2249-555X

Physics

# SPECTRAL ANALYSIS OF ETHYL 6-(CHLOROMETHYL)-4-(3-CHLOROPHENYL)-2-OXO-1,2,3,4-TETRAHYDROPYRIMIDINE-5-CARBOXYLATE– USING DFT COMPUTATIONS

**G. Shakila*** Department of Physics, Bharathidasan Government College for Women, Puducherry-605003, India. *Corresponding author

**H. Saleem** Department of Physics, Annamalai University, Annamalainagar-608002, Tamilnadu, India.

**ABSTRACT** In this work, the FT-IR, FT-Raman spectra, the NMR and UV-Vis spectra of ethyl 6-(chloromethyl)-4-(3-chlorophenyl)-2-oxo-1,2,3,4-tetrahydropyrimidine-5-carboxylate (ECM3CTC) have been recorded and analyzed. All the theoretical parameters in this work have been calculated using DFT at B3LYP/6-311++G(d,p) level. The molecular structures, fundamental vibrational frequencies and intensity of the vibrational bands were investigated theoretically and interpreted comparing with experimental values. The optimized bond parameters of ECM3CTC were compared with X-ray diffraction data of the molecule. The vibrational wavenumber were assigned on the basis of total energy distribution (TED) determined using Veda4 program. Stability of the molecule arising from hyper conjugative interactions, UV transition and charge delocalization was analyzed using natural bond orbital (NBO) analysis. In addition, the 1H and 13C NMR chemical shifts values of ECM3CTC in the ground state were also calculated using Gauge independent atomic orbital (GIAO) method. The docking of the Molecule ECM3CTC was performed by using Glide module implemented in Maestro version 9.3.5 of Schrödinger software suite, 2011.

**KEYWORDS :** FT-IR, FT-Raman, NMR, UV analysis, NBO and Molecular docking studies.

## 1. INTRODUCTION

Pyrimidine nucleus contains two nitrogen atoms at positions 1 and 3 of the six- membered ring. Pyrimidine and its derivatives is the most important heterocyclic aromatic organic compound. It is exhibiting remarkable pharmacological and biological activities, because it is an essential constituent of all cells and thus all living matter **[Sasada et al., 2009]**. Pyrimidine ring is found in cytosine, uracil and thymine which are the essential building blocks of nucleic acids namely DNA and RNA **[Amir et al., 2007].** It is also found in vitamin B2, riboflavin and folic acid **[Stanisaw, 2009]**. They are also found to exhibit remarkable pharmacological activities such as anti-cancer, anti-tumor, anti-microbial, anti-viral, analgesic, anti-HIV, anti-inflammatory and antifungal **[Desai et al., 2006, Amr et al., 2007, Fujiwara et al., 2008 and Wagner et al., 2008]** etc. They are also widely used as agrochemicals, pharmaceuticals, dyes, organic additives in electroplating of steel and in the polymerization process **[Sharma et al., 2014 and Vaisalini et al., 2012].** Many pyrimidine derivatives have been developed as chemotherapeutic agents. Dihydro pyrimidinones, the product of the Biginelli reaction, are also used in the pharmaceutical industry **[Beena et al., 2012]**. Phenyl and its derivatives is biologically and industrially useful compound. They are used in the manufacturing of dyes, drugs, plastics, explosives, pesticides, etc. The inclusion of chlorine with phenyl ring leads to considerable variation of charge distribution in benzene ring and consequently greatly affects the structural, electronic and vibration properties. Generally chlorine or any halogen is referred to as electron withdrawing substituent in the aromatic systems **[Bist et al., 1967 and Evans, 1960]**.

Chlorophenyl has got a variety of uses ranging from preparation of preservatives to insecticides. Thus, Owing to the wide applications and interesting properties of various constituent of the molecule ECM3CTC, a systematic spectral analysis supported by quantum computational methods based on DFT theories has been carried out in the present study. A detailed structural, vibrational, UV-Visible electronic transitional and NMR chemical shift studies have been reported. The non-covalent bonding and anti-bonding interaction can be quantitatively described in terms of the NBO analysis, which is expressed by means of the second-order perturbation interaction energy ($E^{(2)}$). This energy represents the estimation of the off-diagonal NBO Fock matrix elements. It can be deduced from the second-order perturbation approach.

## 2. COMPUTATIONAL DETAILS

The density functional theory (DFT) has been proven to be extremely effective in determining the various physical and chemical properties of the molecules. All the quantum chemical computations in the present work are performed using the Gaussian 09 software programs **[Frisch et al., 2004 and Schlegel, 1982]** on a Pentium IV/3.02GHz personal computer. The Total energy distribution (TED) values are computed for every vibrational modes using VEDA4 program **[Jamroz, 2004]**. The Raman activities were transformed into Raman intensities using *Raint* program **[Michalska, 2003 and Michalska et al., 2005].** The wave numbers and geometrical parameters were computed using B3LYP methods with 6-311++G (d,p) basis set. The geometry corresponding to the real minimum on the potential energy surface (PES) has been obtained and the UV-Visible spectra electronic transition such as HOMO-LUMO excitation energies and oscillator strength were calculated using time-dependent TD-SCF-B3LYP method and also using experimental method. The NMR chemical shift was carried out by GIAO method in B3LYP method with 6-311++G(d,p) basis set. The natural bonding orbital (NBO) computations were done using B3LYP function with 6-311++G(d,p) basis set based on a second-order perturbation theory.

## 3. EXPERIMENTAL DETAILS

### 3.1 Synthesis Procedure

The compound under study was prepared by heating a mixture of ethyl-4-chloroacetoacetate (4.1 ml, 0.025 mol), 3-chlorobenzaldehyde (3.6 g, 0.025 mol), and urea (4.5 g, 0.075 mol) in ethanol (5 ml) under reflux in the presence of concentrated HCl (1 mL) for 8 hrs (monitored by TLC). The reaction mixture, after being cooled to room temperature, was poured onto crushed ice and stirred for 5-10 min. The precipitate was washed with sodium bicarbonate solution, filtered, dried and again washed with petroleum ether (40-60%) and dried over in a vacuum. The compound was recrystallized from absolute ethanol with melting point 151-153º C and yield 72%.The schematic diagram of the title molecule is shown in Fig.1a.

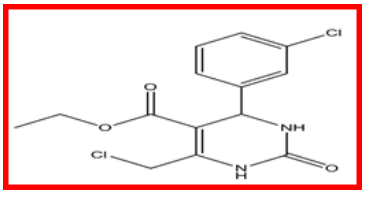


**Fig.1a. Scheme of ECM3CTC**

### 3.2. Spectral measurements

#### 3.2.1. FT-IR, FT-Raman, UV-Vis and NMR Spectra Details

The FTIR spectrum was recorded in the spectral range 4000-400 $cm^{-1}$ using KBr pellet technique with a FTIR-Shimadzu spectrometer. The spectrum was recorded at room temperature with a scanning speed of 10 $cm^{-1}$ per minute with the spectral resolution of 2.0 $cm^{-1}$ at Instrumentation laboratory, Jamal Mohamed College, Tiruchirappalli,

Tamilnadu. FT-Raman spectrum was recorded using Nd:YAG 1064 nm laser as excitation source in the region 4000-50 $cm^{-1}$ on Bruker IFS 66v spectrophotometer equipTED with a FRA 106 FT-Raman module accessory with spectral resolution of 4 $cm^{-1}$ at SAIF Laboratory, IIT Madras. The UV-Vis absorption spectrum of ECM3CTC was recorded in the range of 200-500 nm using a Shimadzu–2600 spectrometer in the department of Chemistry, Jamal Mohamed College, Tiruchirappalli, Tamilnadu. $^{1}H$ NMR spectra were recorded on a Bruker 400 MHz spectrometer and $^{13}C$ NMR spectra were recorded on a Bruker 100 MHz spectrometer in the department of chemistry, Annamalai University, Annamalainagar. Chemical shift values are reported in parts per million (ppm) and tetramethylsilane (TMS) as internal standard.

## 4. RESULTS AND DISCUSSION

### 4.1 Geometrical Analysis

The structure of the ECM3CTC molecule was optimized at B3LYP/6-311++G(d,p) level. Fig. 1b shows the optimized structure of ECM3CTC molecule showing the atom symbols and numbering scheme, respectively. The single crystal X-ray structure for the novel ethyl6-(chloromethyl)-4-(3-chlorophenyl)-2-oxo-1,2,3,4-tetrahydro pyrimidine-5-carboxylate molecule reported at the earlier work **[Bharanidharan et al., 2014]** was used for comparison and analysis. The selected bond parameters such as bond lengths, bond angles and dihedral angles values are presented in Table.1 against the reported XRD data. In this study, the tetrahydropyrimidine ring is found to be almost planar; their bond lengths and bond angles nearly coincide with literature value **[Bharanidharan et al., 2014]**. From the theoretical values, it is found that most of the optimized bond lengths are slightly larger than the experimental values. The CC bond length values inside the pyrimidine ring lies in the range 1.403 Å to 1.374 Å, the corresponding XRD values are 1.357 Å and 1.394 Å, respectively. But the phenyl ring CC values lies in the range 1.38 Å to 1.39 Å. This difference in values indicate the conjugational difference between the pyrimidine and phenyl ring, which shows the electronic distribution inside these two rings are slightly different and there is neither single bonded nor double bonded CC inside these rings. The single bonded C-C has the bond length values lies in the range 1.45 to 1.50 Å, while the double bonded CC values in the range 1.33 to 1.34 Å. The table shows C10-C11 bond length is 1.529 Å and that of C11-C24 is 1.487 Å, which indicates they are purely single bonded but with a different electronic density or distribution. According to the bond length values computed for this molecule, there is no CC bond which is purely double bonded but some of the bonds in the phenyl and pyrimidine rings are closer to double bonded CC, which can be identified through vibrational analysis. The average bond distances of C12–N18 and C14–N18 in the pyrimidine ring calculated by DFT method are 1.403 Å and 1.374 Å, respectively. The breakdown of hexagonal symmetry of the pyrimidine ring is obvious from the shortening of C12–N18 (~0.046 **Å**) and elongation of C14–N18 (~0.019 **Å**) due to the substitution of oxo group to the ring. There is a shortening of C20-Cl23 bond length (~ 0.056 **Å**) and C24-O26 bond length (~ 0.029 **Å**) due to the substitution of chloro methyl group and carboxylate group to the pyrimidine ring.

The asymmetry of the pyrimidine ring is also evident from the negative deviation of C10–C11–C14 (118°) and positive deviation of N16-C12-O17 (125°) from the normal value of 120°. The carbon atoms usually take two types of hybridization $SP^2$ and $SP^3$ when they are in rings, with bond angle 120° and 109° respectively. In this molecule, for many of the bond angles around carbon show the values in the range 118° to 122° both in phenyl and pyrimidine rings which shows the deviation from the $SP^2$ hybridization at these atoms. At H21-C20-H22, H21-C20-CL23) and H22-C20-CL23 the bond angles are 108.4°, 107.4°, 106.6° respectively, this shows the deviation from the $SP^3$ hybridization. It also indicates that the $SP^3$ takes place when there is an H atom on one side of the carbon atom. All these deviation from the ideal angles 120° and 109° indicate that the regular hexagonal structure is distorted due to the substitutional groups and presence of N atoms in the pyrimidine group.

Also, the N18-C12-N16-C10, N16-C12-N18-C14 and O17-C12-N18-C14 dihedral angle is positively (~2.2°), (~3.4°) and (~4.4°) deviated from the corresponding XRD values. The O17-C12-N16-C10 dihedral angle is negatively (~4.1°) deviated from the corresponding XRD value. This deviation is mainly due to the substitution of oxo group and chloro methyl group to the ring. The C10-C1-C2-C3 dihedral angle is positively (~1.1°) deviates from the corresponding XRD value is due to the substitution of chloro phenyl group to the ring. The carboxylate group C11-C24-O26-C27 dihedral angle parameter is positively (~2.5°) deviated with reported XRD value, due to the reason for the crystal disorder over two positions in ethyl group.

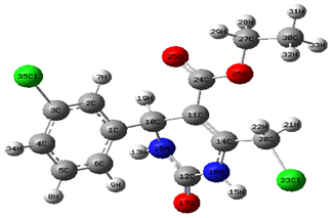

**Fig. 1b. Optimized structure of ECM3CTC**

**Table 1. The selected bond parameters of ECM3CTC**

| Bond Parameters | B3LYP/6-311++G(d,p) | XRD[a] |
|---|---|---|
| **Bond Lengths (Å)** | | |
| C1-C2 | 1.4026 | 1.351 |
| C1-C6 | 1.3997 | 1.381 |
| C1-C10 | 1.5387 | 1.526 |
| C2-C3 | 1.3917 | 1.354 |
| C3-C4 | 1.3943 | 1.381 |
| C3-CL35 | 1.7617 | 1.723 |
| C4-C5 | 1.3933 | 1.364 |
| C5-C6 | 1.396 | 1.358 |
| C10-C11 | 1.529 | 1.503 |
| C10-N16 | 1.4622 | 1.482 |
| C11-C24 | 1.4666 | 1.487 |
| C12-N16 | 1.3663 | 1.333 |
| C12-O17 | 1.2203 | 1.228 |
| C12-N18 | 1.4036 | 1.357 |
| C14-N18 | 1.3744 | 1.394 |
| C20-CL23 | 1.8167 | 1.76 |
| C24-O25 | 1.2221 | 1.205 |
| O26-C27 | 1.4496 | 1.46 |
| **Bond Angles (°)** | | |
| C2-C1-C6 | 119.1487 | 122.3 |
| C1-C2-C3 | 119.5599 | 117.8 |
| C2-C3-C4 | 121.7374 | 121.6 |
| C3-C4-C5 | 118.3725 | 119.6 |
| C4-C5-C6 | 120.8042 | 119.9 |
| C1-C6-C5 | 120.3738 | 118.8 |
| C1-C10-N16 | 113.2246 | 110.7 |
| C11-C10-N16 | 108.5973 | 108.6 |
| N16-C12-O17 | 125.3629 | 123 |
| O17-C12-N18 | 121.0855 | 121.3 |
| C10-N16-C12 | 123.148 | 123.8 |
| O25-C24-O26 | 121.9093 | 122.4 |
| **Dihedral Angles (°)** | | |
| C6-C1-C2-C3 | 0.6511 | 1.0 |
| C10-C1-C2-C3 | -179.0294 | -177.9 |
| C10-C1-C6-C5 | 179.0242 | 179.0 |
| O17-C12-N16-C10 | 160.2809 | 164.3 |
| N18-C12-N16-C10 | -21.6273 | -19.4 |
| N16-C12-N18-C14 | -9.4486 | -6.0 |
| O17-C12-N18-C14 | 168.7343 | 164.3 |
| C11-C24-O26-C27 | 179.8018 | 177.3 |

[a]Bharanidharan et al., J.New developments in chem.., 1:2 (2016) 1-25.

### 4.2 Vibrational Investigations

The title molecule under investigation has 35 number of atoms and 99 normal modes of fundamental vibrations, which can be distributed using the irreducible representations as $\Gamma_{Vib} = 67\ A' + 32\ A''$. All the vibrations are found active collectively in both IR and Raman spectra. The assignments of all the fundamentals have been made on the basis of TED values along with the comparison of available literature on the structurally similar molecules. The calculated wave numbers are found slightly higher than the observed values for the majority of the normal

modes. Two factors may be responsible for the discrepancies between the experimental and computed wave numbers; the first is caused by the unpredictable electronic distribution among the different bonds in the molecule and the second reason is the anharmonic nature of the vibrations **[Scott et al., 1996]** which cannot be accounted completely by theory. Scaling strategies were used to bring computed wave numbers coincide with observed values. In this, study, the scaling factor used is 0.9608 as advised by the earlier work **[Radom et al., 1970].** The intensities, reduced mass and Force constants along with the wave numbers and assignment are presented in Table 2. The theoretical and experimental IR and Raman spectra are also constructed and shown in Figs. 2 & 3.

### 4.2.1 CH vibrations

In the aromatic compounds, the C-H stretching normally occurs in the region of 3100–3000 $cm^{-1}$ **[Michalska, 2003].** For the title molecule, the C-H stretching vibrations of chloro phenyl group are observed at 3228, 3119 $cm^{-1}$ in IR region and 3075 $cm^{-1}$ in Raman (mode: 3, 4. 7). The corresponding calculated values occur at 3228, 3223 and 3193 $cm^{-1}$. This observation indicates that all the stretching vibrations are in the higher range and this is due to the considerable impact of substitution on the rings. Especially the bands are predominated by the Cl atom in the phenyl ring. The scaled harmonic frequencies in the range 3139-3056 $cm^{-1}$ (mode nos: 8,9,11, 13, 14) are attributed to C-H stretching vibrations of carboxylate group attached to the pyrimidine ring in ECM3CTC. All these mixing modes are observed in the FT-Raman spectrum and all these vibrations are in the lower range due to the impact of O atom in the carboxylate group. The pure mode of wave number 2972 $cm^{-1}$ in the FT-Raman spectrum (mode 12) with TED 99% contributionis due to the C-H stretching vibration of the pyrimidine ring. This mode is shifted to the lower wave number region due to the substitution of chloro phenyl group in the adjacent position. The corresponding computed unscaled value is 3097 $cm^{-1}$ and this coincides with the assignment made by Alam et al. **[Alam et al., 2016].** The theoretically calculated values of C-H in-plane bending vibrations of phenyl ring fall in the region 1519-1198 $cm^{-1}$ (mode nos: 21, 32, 39, 41).Similarly the harmonic bands due to C-H out-of-plane bending vibration fall in the region 985-790 $cm^{-1}$ (mode nos: 51, 54, 59, 61). In this study, some of the experimental bands are slightly higher for $\beta_{CH}$ mode, which may be due to the steric factor of bulky group (pyrimidine ring). In general, the $\beta_{CH}$ and $\tau_{CH}$ modes are within the expected region with few exceptions and also having considerable TED values: >20 and mode no: 54 is a pure out-of-plane bending mode with TED 79%, respectively..

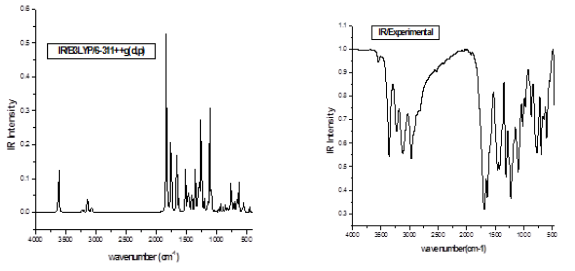


**Fig. 2. The combined theoretical and experimental FT-IR Spectra of ECM3CTC**

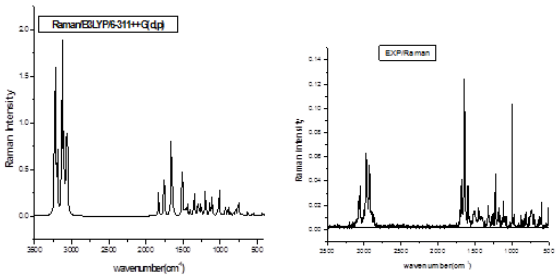


**Fig. 3. The combined theoretical and experimental FT-Raman Spectra of ECM3CTC**

**Table 2. The experimental and calculated frequencies of ECM3CTC using B3LYP/6-311++G(d,p) level of basis set [harmonic frequencies ($cm^{-1}$), IR, Raman intensities (Km/mol), reduced masses (amu) and force constants ($mdynA^{\circ -1}$)]**

| Mode No. | Calculated Frequencies ($cm^{-1}$) | | Observed Frequencies ($cm^{-1}$) | | IR Intensity | | Raman Intensity | | Reduced Masses | Force Constants | Vibrations Assignments≥10% (TED)[d] |
|---|---|---|---|---|---|---|---|---|---|---|---|
| | Un Scaled | Scaled[a] | IR | Raman | Rel.[b] | Abs. | Rel.[c] | Abs. | | | |
| 1 | 3631 | 3511 | 3544 | | 38.75 | 6.93 | 31.00 | 2.24 | 1.08 | 8.37 | νN16H13(100) |
| 2 | 3613 | 3493 | 3360 | | 153.45 | 27.46 | 27.56 | 1.99 | 1.08 | 8.29 | νN18H15(100) |
| 3 | 3228 | 3121 | 3228 | | 5.83 | 1.04 | 21.90 | 1.58 | 1.09 | 6.70 | VC2H7(99) |
| 4 | 3223 | 3116 | 3119 | | 4.76 | 0.85 | 72.55 | 5.23 | 1.10 | 6.71 | VC4H34(79)+VC5H8(11) |
| 5 | 3216 | 3109 | | | 3.30 | 0.59 | 15.63 | 1.13 | 1.09 | 6.65 | VC4H34(14)+VC6H9(81) |
| 6 | 3212 | 3106 | | | 0.14 | 0.03 | 13.85 | 1.00 | 1.10 | 6.70 | VC20H21(15)+VC20H22(84) |
| 7 | 3193 | 3087 | | 3075 | 6.89 | 1.23 | 36.11 | 2.60 | 1.09 | 6.53 | VC5H8(84)+VC6H9(10) |
| 8 | 3139 | 3034 | | 3056 | 35.63 | 6.38 | 5.53 | 0.40 | 1.11 | 6.42 | VC27H28(13)+VC27H29(13)+VC30H32(36)+VC30H33(37) |
| 9 | 3132 | 3028 | | | 21.81 | 3.90 | 50.82 | 3.67 | 1.10 | 6.37 | VC30H31(67)+VC30H32(16)+VC30H33(15) |
| 10 | 3128 | 3024 | | | 4.28 | 0.77 | 48.86 | 3.52 | 1.07 | 6.14 | VC20H21(84)+VC20H22(15) |
| 11 | 3112 | 3009 | | | 1.97 | 0.35 | 40.87 | 2.95 | 1.11 | 6.32 | VC27H28(37)+VC27H29(36)+VC30H32(14)+VC30H33(13) |
| 12 | 3097 | 2994 | | 2972 | 3.81 | 0.68 | 28.85 | 2.08 | 1.09 | 6.14 | $\nu C_{10}H_{19}$(99) |
| 13 | 3073 | 2971 | 2973 | 2928 | 15.79 | 2.83 | 41.94 | 3.02 | 1.06 | 5.89 | VC27H28(48)+VC27H29(50) |
| 14 | 3056 | 2954 | | 2872 | 13.86 | 2.48 | 68.83 | 4.96 | 1.04 | 5.70 | VC30H31(32)+VC30H32(34)+VC30H33(34) |
| 15 | 1831 | 1770 | 1924 | | 558.88 | 100.00 | 46.47 | 3.35 | 7.96 | 15.73 | VO17C12(72)+βN16C12N18(11) |
| 16 | 1756 | 1698 | 1692 | 1683 | 347.18 | 62.12 | 125.07 | 9.02 | 12.17 | 22.11 | VO25C24(86) |

| | | | | | | | | | | | |
|---|---|---|---|---|---|---|---|---|---|---|---|
| 17 | 1660 | 1605 | 1640 | 1645 | 163.77 | 29.30 | 158.91 | 11.46 | 8.54 | 13.87 | VC11C14(66) |
| 18 | 1648 | 1593 | | 1597 | 25.73 | 4.60 | 86.57 | 6.24 | 5.93 | 9.49 | VC4C3(17)+VC6C5(28)+βC 5C4C3(12) |
| 19 | 1628 | 1574 | | | 39.21 | 7.02 | 21.22 | 1.53 | 5.70 | 8.90 | VC5C4(52)+VC1C6(54)+βC 4C3C2(35) |
| 20 | 1532 | 1481 | | | 2.86 | 0.51 | 2.77 | 0.20 | 1.09 | 1.51 | βH28C27H29(54)+βH32C30 H33(16)+ΓC27H28C30H29(1 7) |
| 21 | 1519 | 1469 | | | 40.56 | 7.26 | 3.81 | 0.27 | 2.24 | 3.05 | βH7C2C3(20)+βH8C5C4(31) +βH9C6C5(10) |
| 22 | 1511 | 1461 | | 1508 | 1.77 | 0.32 | 48.34 | 3.49 | 1.05 | 1.41 | βH28C27H29(32)+βH32C30 H33(42) |
| 23 | 1509 | 1459 | 1458 | 1456 | 113.23 | 20.26 | 58.01 | 4.18 | 2.39 | 3.21 | vN18C14(26)+ βH15N18C14(44) |
| 24 | 1502 | 1452 | | | 6.79 | 1.22 | 55.57 | 4.01 | 1.04 | 1.38 | βH31C30H32(65)+τH32C30C 27O26(14)+τH33C30C27O26 (10) |
| 25 | 1474 | 1425 | 1424 | | 66.09 | 11.83 | 20.91 | 1.51 | 2.19 | 2.81 | βH13N16C10(10)+βH9C6C5( 13)+ΓC10C1C11H19(21) |
| 26 | 1464 | 1415 | | | 32.30 | 5.78 | 11.68 | 0.84 | 1.15 | 1.45 | βH21C20H22(82) |
| 27 | 1453 | 1405 | | | 44.74 | 8.00 | 10.15 | 0.73 | 1.91 | 2.37 | βH13N16C10(35) |
| 28 | 1439 | 1391 | | | 11.75 | 2.10 | 32.37 | 2.33 | 1.41 | 1.72 | βH31C30C27(23)+βH32C30 H33(13)+ΓC27H28C30H29(2 1)+TH33C30C27O26(10) |
| 29 | 1408 | 1361 | | | 6.28 | 1.12 | 5.20 | 0.38 | 1.55 | 1.81 | βH31C30C27(17)+βH32C30 H33(15)+ΓC27H28C30H29(2 9) |
| 30 | 1406 | 1360 | 1374 | | 62.53 | 11.19 | 16.71 | 1.21 | 1.97 | 2.29 | vN16C12(12)+vN18C12(11)+ βH13N16C10(23)+ΓC10C1C1 1H19(14) |
| 31 | 1358 | 1313 | 1310 | 1323 | 48.67 | 8.71 | 16.90 | 1.22 | 2.36 | 2.56 | VC4C3(21)+VC1C6(13)+βH 19C10C1(39) |
| 32 | 1351 | 1306 | | | 16.45 | 2.94 | 9.63 | 0.69 | 1.50 | 1.61 | βH7C2C3(26)+βH34C4C5(18 )+βH9C6C5(10)+βH19C10C1 (20) |
| 33 | 1347 | 1302 | | | 126.39 | 22.61 | 76.47 | 5.52 | 3.56 | 3.80 | VC24C11(19)+ΓC27H28C30 H29(15) |
| 34 | 1308 | 1265 | | 1275 | 52.32 | 9.36 | 17.41 | 1.26 | 1.35 | 1.36 | ΓC20H22C14H21(53) |
| 35 | 1301 | 1258 | | | 26.84 | 4.80 | 4.97 | 0.36 | 1.77 | 1.77 | VC4C3(13)+VC1C6(19) |
| 36 | 1297 | 1254 | | 1256 | 1.77 | 0.32 | 42.74 | 3.08 | 1.10 | 1.09 | βH28C27C30(77) |
| 37 | 1285 | 1243 | | | 130.45 | 23.34 | 32.79 | 2.37 | 2.28 | 2.22 | vN18C14(20)+βH15N18C14( 31) |
| 38 | 1257 | 1215 | 1226 | 1225 | 392.99 | 70.32 | 62.50 | 4.51 | 2.23 | 2.08 | ΓC10C1C11H19(25) |
| 39 | 1206 | 1166 | | 1193 | 15.28 | 2.73 | 15.28 | 1.10 | 1.34 | 1.15 | βH8C5C4(21)+βH9C6C5(26) |
| 40 | 1202 | 1162 | | 1172 | 6.34 | 1.13 | 39.90 | 2.88 | 1.09 | 0.93 | βH22C20C14(70)+ΓC20H22 C14H21(11) |
| 41 | 1198 | 1158 | | | 27.67 | 4.95 | 62.16 | 4.48 | 2.10 | 1.77 | VC6C5(15)+βC2C1C6(13)+ VC1C10(20)+βH34C4C5(11) + βH8C5C4(13) |
| 42 | 1183 | 1144 | | | 3.52 | 0.63 | 7.84 | 0.57 | 1.53 | 1.26 | βH31C30H32(14)+ΓC27C30 O26H28(18)+τH28C27C30H3 1(36)+TH32C30C27O26(22) |
| 43 | 1149 | 1111 | | 1119 | 23.48 | 4.20 | 15.13 | 1.09 | 2.40 | 1.86 | $vO_{26}C_{24}(10)$+ $vN_{16}C_{10}(18)$+ $vC_{10}C_{11}(16)$ |
| 44 | 1140 | 1102 | 1099 | | 4.43 | 0.79 | 48.04 | 3.46 | 2.22 | 1.70 | $vC_{27}C_{30}(18)$+ $\beta H_{31}C_{30}H_{27}(16)$+ $\beta C_{30}C_{27}O_{26}(15)$+$\tau H_{32}C_{30}C_{27}O_{26}(1$ 4)+ $\tau H_{33}C_{30}C_{27}O_{26}(14)$ |
| 45 | 1124 | 1087 | | | 9.08 | 1.62 | 5.80 | 0.42 | 1.68 | 1.25 | βH34C4C5(27)+βC4C3C2(10 ) |
| 46 | 1113 | 1076 | | 1080 | 59.51 | 10.65 | 36.28 | 2.62 | 2.24 | 1.64 | VC5C4(19)+VC6C5(10)+βC 4C3C2(15) |
| 47 | 1112 | 1075 | | | 280.51 | 50.19 | 56.83 | 4.10 | 5.71 | 4.16 | VO26C24(20)+VC20C14(12) +VO26C27(12) |
| 48 | 1087 | 1051 | | | 65.49 | 11.72 | 12.92 | 0.93 | 3.82 | 2.66 | vN16C10(13)+VC11C10(15) |
| 49 | 1037 | 1002 | 1018 | 999 | 6.69 | 1.20 | 16.09 | 1.16 | 2.93 | 1.85 | VC30C27(45)+VO26C27(18) |
| 50 | 1012 | 979 | 972 | 973 | 2.28 | 0.41 | 164.77 | 11.88 | 6.15 | 3.71 | βC1C2C3(19)+VC6C5(10)+β C6C5C4(29) |

| | | | | | | | | | | | |
|---|---|---|---|---|---|---|---|---|---|---|---|
| 51 | 985 | 952 | | | 0.01 | 0.00 | 2.06 | 0.15 | 1.30 | 0.74 | τH34C4C5C6(13)+ΓC5C4C6H8(62)+τH9C6C5C4(20) |
| 52 | 965 | 933 | | | 18.24 | 3.26 | 13.93 | 1.00 | 3.71 | 2.04 | νN16C12(16)+ν18C12(29)+VC20C14(14) |
| 53 | 933 | 902 | | | 6.59 | 1.18 | 33.13 | 2.39 | 1.77 | 0.91 | ΓC20C14Cl23H 22(74)+ΓC20C11N18C14(10) |
| 54 | 928 | 897 | | | 21.14 | 3.78 | 28.42 | 2.05 | 1.45 | 0.74 | ΓC2C1C3H7(79) |
| 55 | 919 | 888 | | 877 | 1.68 | 0.30 | 4.25 | 0.31 | 1.36 | 0.68 | τH34C4C5C6(43)+τH9C6C5C4(44) |
| 56 | 893 | 863 | 867 | | 20.34 | 3.64 | 61.63 | 4.44 | 2.82 | 1.33 | VC30C27(10)+VO26C27(27)+βH31C30C27(14) |
| 57 | 869 | 840 | | 841 | 3.93 | 0.70 | 22.78 | 1.64 | 4.36 | 1.94 | VO26C24(10)+VC1C10(12)+βC5C4C3(12) |
| 58 | 853 | 824 | | 810 | 24.88 | 4.45 | 21.41 | 1.54 | 6.51 | 2.79 | βO25C24O26(12)+βN16C12N18(10) |
| 59 | 823 | 796 | | | 18.15 | 3.25 | 22.20 | 1.60 | 2.80 | 1.12 | τH34C4C5C6(11)+ΓC1C11N16C10(18) |
| 60 | 813 | 786 | | | 0.52 | 0.09 | 3.47 | 0.25 | 1.12 | 0.44 | βH28C27C30(12)+ΓC27C30O26H28(66) |
| 61 | 790 | 763 | 769 | 770 | 13.50 | 2.42 | 42.27 | 3.05 | 1.94 | 0.71 | τH34C4C5C6(15)+ΓC5C4C6H8(19)+τH9C6C5C4(14) |
| 62 | 766 | 740 | | | 17.90 | 3.20 | 32.86 | 2.37 | 7.26 | 2.51 | ΓO25C11O26C24(50)+ΓO17N16N18C12(10) |
| 63 | 761 | 735 | | | 72.56 | 12.98 | 44.07 | 3.18 | 7.82 | 2.67 | VCl23C20(21)+ΓO25C11O26C24(10)+ΓO17N16N18C12(30) |
| 64 | 747 | 722 | | 739 | 37.70 | 6.75 | 119.99 | 8.65 | 7.48 | 2.46 | VCl23C20(16)+ΓO17N16N18C12(48) |
| 65 | 715 | 691 | 696 | | 16.44 | 2.94 | 19.02 | 1.37 | 3.20 | 0.96 | τC1C6C4C5(15)+ΓO25C11O26C24(11) |
| 66 | 703 | 679 | | 703 | 35.07 | 6.27 | 18.38 | 1.33 | 4.41 | 1.28 | βC6C5C4(12)+τC3C2C4C5(10)+τC1C6C4C5(14) |
| 67 | 675 | 653 | 663 | | 8.75 | 1.57 | 12.81 | 0.92 | 3.79 | 1.02 | βN16C12N18(15)+τH15N18C14C11(13)+τC3C2C4C5(10) |
| 68 | 656 | 634 | 642 | 633 | 58.35 | 10.44 | 10.55 | 0.76 | 2.68 | 0.68 | βO25C24O26(10)+βN16C12N18(10)+τH13N16C12N18(10)+ τH15N18C14C11(22) |
| 69 | 630 | 610 | | | 83.91 | 15.01 | 28.71 | 2.07 | 2.00 | 0.47 | τH13N16C12N18(12)+τH15N18C14C11(32) |
| 70 | 624 | 604 | 600 | 602 | 10.05 | 1.80 | 38.09 | 2.75 | 5.31 | 1.22 | VCl23C20(13)+βC1C10N16(11)+τC3C2C4C5(12) |
| 71 | 565 | 546 | 542 | | 18.90 | 3.38 | 27.12 | 1.96 | 1.51 | 0.28 | τH13N16C12N18(47)+τH15N18C14C11(19) |
| 72 | 549 | 531 | | | 15.57 | 2.79 | 16.89 | 1.22 | 3.96 | 0.70 | βC11C14N18(14)+ΓC20C11N18C14(13) |
| 73 | 548 | 530 | | | 10.87 | 1.95 | 21.35 | 1.54 | 3.84 | 0.68 | βC11C14N18(14)+βC11C10N16(11)+ΓC20C11N18C14(12) |
| 74 | 525 | 508 | | 512 | 6.92 | 1.24 | 18.33 | 1.32 | 4.06 | 0.66 | βN18C12O17(13)+βN16C12N18(14) |
| 75 | 453 | 438 | 456 | | 10.21 | 1.83 | 1.08 | 0.08 | 3.51 | 0.42 | τC4C3C5C6(36)+τC1C6C4C5(17) |
| 76 | 447 | 432 | | 424 | 9.11 | 1.63 | 6.72 | 0.48 | 6.02 | 0.71 | βN18C12O17(27)+βO26C24C11(18)+βC30C27O26(12) |
| 77 | 427 | 413 | | | 2.52 | 0.45 | 50.83 | 3.67 | 7.84 | 0.84 | VCl35C3(41)+βC5C4C3(10) |
| 78 | 392 | 379 | | | 7.12 | 1.27 | 43.07 | 3.11 | 4.62 | 0.42 | βO25C24O26(22)+βC30C27O26(31) |
| 79 | 378 | 365 | | 364 | 0.32 | 0.06 | 111.86 | 8.07 | 5.47 | 0.46 | βC4C3Cl35(14) |
| 80 | 356 | 345 | | | 2.24 | 0.40 | 36.24 | 2.61 | 6.48 | 0.49 | βC2C1C6(10)+βC11C10N16(10)+βC4C3Cl35(22) |
| 81 | 321 | 310 | | | 17.97 | 3.22 | 49.18 | 3.55 | 7.72 | 0.47 | βO26C24C11(10)+βC27O26C24(18)+βCl23C20C14(12) |
| 82 | 302 | 292 | | | 0.63 | 0.11 | 55.07 | 3.97 | 5.67 | 0.31 | VC1C10(11)+βC6C1C10(11)+ βC1C10N16(11)+βC4C3Cl35(16) |
| 83 | 288 | 278 | | | 1.38 | 0.25 | 58.94 | 4.25 | 6.57 | 0.32 | VC24C11(12)+βC1C10N16(14)+βC27O26C24(11)+βCl23C20C14(10) |
| 84 | 270 | 261 | | | 1.05 | 0.19 | 9.90 | 0.71 | 1.28 | 0.06 | τH28C27C30H31(40)+τH33C30C27O26(33) |
| 85 | 227 | 220 | | | 3.67 | 0.66 | 55.93 | 4.03 | 6.06 | 0.18 | βC10C11C24(29)+βC30C27O26(11) |
| 86 | 216 | 209 | | 201 | 1.69 | 0.30 | 113.83 | 8.21 | 4.59 | 0.13 | τC3C2C4C5(14)+τC4C3C5C6(12)+τC1C6C4C5(13)+ΓC24C10C14C11(11) |
| 87 | 193 | 187 | | | 2.82 | 0.51 | 25.94 | 1.87 | 5.47 | 0.12 | τC1C2C3Cl35(60) |
| 88 | 172 | 167 | | 166 | 1.71 | 0.31 | 44.89 | 3.24 | 9.68 | 0.17 | βC11C14C20(40)+βCl23C20C14(26) |
| 89 | 160 | 155 | | | 2.51 | 0.45 | 151.81 | 10.95 | 5.77 | 0.09 | βC6C1C10(16)+βC4C3Cl35(10)+τC12N18C11C14(18) |
| 90 | 154 | 149 | | | 1.22 | 0.22 | 93.90 | 6.77 | 4.72 | 0.07 | βC6C1C10(17)+βC4C3C35(11)+τC12N18C11C14(39)+ΓC20C11N18C14(10) |
| 91 | 128 | 123 | | | 1.73 | 0.31 | 3.49 | 0.25 | 3.16 | 0.03 | τC27O26C24C11(57) |
| 92 | 105 | 101 | | | 0.69 | 0.12 | 18.93 | 1.37 | 6.13 | 0.04 | τC14C11C24O26(44)+τC30C27O26C24(12) |
| 93 | 94 | 91 | | 90 | 0.18 | 0.03 | 25.15 | 1.81 | 5.11 | 0.03 | βO26C24C11(23)+βC10C11C24(18)+βC27O26C24(19) |
| 94 | 75 | 72 | | | 0.56 | 0.10 | 134.42 | 9.69 | 5.78 | 0.02 | τC10N16N18C12(57)+ΓC24C10C14C11(10) |
| 95 | 65 | 63 | | | 3.02 | 0.54 | 394.63 | 28.46 | 3.94 | 0.01 | τC10N16C11C14(30)+τN18C14C20Cl23(13)+ΓC1C11N16C10(11) |
| 96 | 57 | 55 | | | 0.29 | 0.05 | 250.21 | 18.04 | 3.17 | 0.01 | τC30C27O26C24(47) |
| 97 | 32 | 31 | | | 0.03 | 0.01 | 776.69 | 56.01 | 4.49 | 0.00 | TC14C11C24O26(10)+τC30C27O26C24(24)+τN18C14C20Cl23(16) |
| 98 | 19 | 19 | | | 0.53 | 0.09 | 1095.91 | 79.03 | 6.20 | 0.00 | τC6C1C10C11(56)+τC14C11C24O26(11)+τN18C14C20Cl23(10) |
| 99 | 9 | 9 | | | 0.96 | 0.17 | 1386.68 | 100.00 | 10.30 | 0.00 | τC6C1C10C11(17)+τC10N16C11C14(20)+τN18C14C20Cl23(38) |

[v]: Stretching, β: in-plane-bending, Γ: out-of-plane bending, τ- Torsion, vw: very week, w: week, m: medium, s: strong, vs: very strong.
[a]Scaling factor: 0.9608 (Random et al., 1970 and Pople et al., 1993).
[b]Relative IR absorption intensities normalized with highest peak absorption equal to 100.

[c] Relative Raman intensities calculated by Equation (1) and normalized to 100.

[d]Total energy distribution calculated at B3LYP/6-311++G(d,p) level.

#### 4.2.2. C-Cl Vibrations

Most aromatic chlorine compounds absorb strongly in the region 600-800 $cm^{-1}$ due to C-Cl stretching vibrations, when there is more than one chlorine atoms on the same ring. The vibrations due to a chlorine atom is worth to discuss since mixing of the vibrations are possible due to lowering of the molecular symmetry and the presence of heavy atom **[Mooney, 1964, Mooney, 1963]**. **[Sundaraganesan et al., 2008]** reported C-Cl stretching at 704 (FT-IR), 705 (Raman), and 715 $cm^{-1}$ (DFT) and the deformation bands at 250 and 160 $cm^{-1}$. In present case, the band observed at 739$cm^{-1}$ in FT-Raman spectrum is assigned as C-Cl stretching of chloro methyl group and the corresponding theoretical wavenumber at 747 $cm^{-1}$. Sundaraganesan et al. reported the C-Cl in-plane and out-of-plane bending deformation bands at 250 and 160 $cm^{-1}$, respectively **[Sundaraganesan et al., 2008].** In this study, the C−Cl in-plane bending vibrations of chloro phenyl ring were calculated at 378, 302 $cm^{-1}$ and that of chloro methyl group at 288, 172 $cm^{-1}$. Similarly, the C−Cl out-plane bending vibrations of chloro phenyl ring and that of chloro methyl group were calculated at 193 & 65 and 32 & 19 $cm^{-1}$respectively.

#### 4.2.3. C-N Vibrations

Generally the C=N/C-N stretching vibrations were observed in the regions of 1600-1670 $cm^{-1}$/1266-1382 $cm^{-1}$ **[Socrates, 2001, Silverstein et al., 1998]** respectively. Khalaji et al. reported that the C=N (aromatic) stretching mode appeared in the region 1490-1570 $cm^{-1}$**[Khalaji et al., 2009]**. For the title molecules, the four C-N stretching vibrations are identified with the help of TED. The CN stretching vibrations are assigned to harmonic wavenumbers 1509, 1406, 1285, 1149 $cm^{-1}$(mode nos: 23, 30, 37, 43). The observed bands occurred in FTIR spectra at 1458 (1456: FT-Raman), 1374, 1119 $cm^{-1}$respectively. These assignments are supported by their TED values. The assignment of CN stretching modes in this molecule indicate that the CN is single bonded rather than double bonded, as the wave number lies in the lower range. The in-plane bending vibrations: $\beta C_7C_{10}N_{16;}$ $\beta C_{11}C_{14}N_{18}$; $\beta N_{16}C_{12}N_{18}$ are attributed to mode nos: 70, 72, 73, 74, 67 and 68 respectively. The out-of-plane bending mode of $\Gamma_{C\text{-}N}$ contributes as mixed vibrations of $\Gamma O_{17}N_{16}N_{18}C_{12}$ and $\Gamma C_{20}C_{11}N_{18}C_{14}$ (mode nos: 63, 90).

#### 4.2.4. C-O Vibrations

The carboxylate C=O stretching mode of ester group **[Roeges, 1994 and Colthup et al., 1975]** is expected to occur in the region 1750-1600 $cm^{-1}$and for ECM3CTC, this mode is observed with very strong band at 1692 $cm^{-1}$ in FT-IR spectrum and 1683 $cm^{-1}$ in FT-Raman. The theoretically calculated wavenumber at 1756 $cm^{-1}$ (mode no. 16) corresponds to C=O stretching vibration mode which is pure mode with TED contribution of 86%. In C-O group, the absorption is sensitive for both the carbon and oxygen atoms. Normally the C–O stretching vibration occurs in the region 1000-1260 $cm^{-1}$. **[Meganathan et al. 2010]** have assigned at 1251 $cm^{-1}$ (FTIR) and 1248 $cm^{-1}$ (FT-Raman) to above mentioned band. The intensity of the carboxylate group increases, due to the conjugation (or) formation of hydrogen bonds. The increase in conjugation, which increase the intensity of Raman lines as well as the IR band intensities **[Varghese et al., 2009].** According to the above facts, the harmonic frequencies 1149, 1112, 1037 (mode nos: 43, 47, 49) are designated as $\nu C_{24}\text{-}O_{26}$, $\nu C_{27}\text{-}O_{26}$ modes, respectively with small TED values (10, 20, 18%) as well as relative IR intensities (23.48, 280.51, 6.69). Further the mode no: 43 appeared as FT-Raman band: 1119 $cm^{-1}$ with medium intensity and mode no: 49 appeared in both FT-IR and FT-Raman region. The in-plane bending vibrations of $\beta_{C\text{-}O}$ are observed as mixed vibration of $\beta C_{27}C_{30}O_{26}$ at 424 $cm^{-1}$ in FT-Raman spectrum, whereas the calculated frequencies are: 447, 392 (mode nos: 76, 78).The C-O out-of-plane bending modes are also contribute as mixed vibration of $\Gamma C_{14}C_{11}C_{24}O_{26}$, and τC14C11C24O26, but shifted to low wave number value due to the substitution of chloro phenyl group in the adjacent position.

#### 4.2.5. CC Vibrations

The ring stretching vibrations are very much important and are characteristic of the phenyl and pyrimidine rings. The C=C stretching vibrations were reported in the regions of 1590-1625, and C-C in the region 1280-1380 $cm^{-1}$ with variable intensity by **[Varsanyi, 1973]**. In this study, the bands observed at 1597, 1323, 1080 $cm^{-1}$ in FT-Raman and at 1310 $cm^{-1}$ in FT-IR spectra are attributed to C=C/C-C stretching mode of phenyl ring in ECM3CTC and their corresponding harmonic frequencies are: 1648, 1628, 1358, 1301, 1198, 1113 $cm^{-1}$ (mode nos : 18, 19, 31, 35, 41, 46). As it is evident from Table the TED value corresponding to all $\nu_{C\text{-}C}$ modes lie in between 12 and 54% and also mixed with $\beta_{CH}$ mode. The wavenumbers for in-plane bending modes of phenyl group are determined experimentally at 1080, 973, 841, 703 $cm^{-1}$ in FT-Raman spectrum and 972 $cm^{-1}$ in FT-IR spectrum. The theoretically computed wave numbers by DFT method are at 1113, 1012, 869, 703 $cm^{-1}$[**Sarojini et al., 2013]**. The modes: 65, 67, 70, 75 at 696, 663, 600, 456 $cm^{-1}$ (FTIR) respectively were recognized as torsional deformation $\tau_{CCC}$modes.

**[Alam et al., 2016]** assigned the C-C stretching vibrations of pyrimidine derivatives in the wavenumber range 1180-1771$cm^{-1}$ (FTIR). The theoretically calculated $\nu_{C\text{-}C}$ modes:1660-1087 $cm^{-1}$ (mode nos: 17, 33, 41, 43, 47, 48, 52) of the pyrimidine ring have been obtained to be consistent with the recorded spectral values:1640, 1428, 1365, 1212 $cm^{-1}$ (FTIR bands) and 1645, 1119 $cm^{-1}$ (FT-Raman).The harmonic wave numbers of $\beta_{CCC}$ and $\Gamma_{CCC}$ modes of pyrimidine ring were computed at 302, 227,172 and 216,75 $cm^{-1}$ respectively. Compared to the above literature values **[Alam et al., 2016]**, these harmonic wave numbers are shifted to the lower range due to the presence of chloro phenyl, carboxylate group and chloro methyl group to the tetra hydro perimidine ring. According to TED results the $\beta_{CCC}$ and $\Gamma_{CCC}$ vibrations are mixed with $\beta_{CCH,}\beta_{CCN}$ and $\tau_{CCH}$,$\tau_{CCN}$ modes of the neighbouring group.

#### 4.2.6. N-H Vibrations

The N-H stretching vibrations usually appear in the region of 3500-3300 $cm^{-1}$ for heterocyclic molecules **[Socrates, 2001]**. In the present molecule the observed vibrational wave numbers at 3544, 3360 $cm^{-1}$ in FTIR spectra and its corresponding calculated values are at 3631, 3613 $cm^{-1}$(mode nos: 1 & 2) are assigned to νN–H mode. These modes are in expected region and also find support from TED value (100%). The observed wave numbers are negatively (87 and 253 $cm^{-1}$) deviated from harmonic frequencies, which is due to the presence of moderate anharmonicity in this vibration. It may also be due to hydrogen-bonding interactions occur within the molecule **[Alam et al., 2016]**. The N-H in-plane bending $\beta_{NH}$ vibration is an important mode, which shows their presence as medium to strong bands in the region 1520-1549 $cm^{-1}$ **[Socrates, 2001]**. In the present molecule, when nitrogen and hydrogen move in opposite with respect to carbon atom the peak observed is at 1458, 1424, 1374 $cm^{-1}$ in FT-IR and 1456 $cm^{-1}$ in FT-Raman band, while the corresponding harmonic wave number at 1509, 1474 and 1406 $cm^{-1}$ (mode nos: 23, 25, 30) are assigned to βNH vibration. Similarly, when the N and H atoms move in same direction it is observed near 1250 $cm^{-1}$ **[Dhandapani et al., 2014]**. In ECM3CTC, the N-H in-plane bending mode βH15N18C14 is calculated at 1285 $cm^{-1}$ and the corresponding experimental band is absent. The N-H torsional mode $\tau H_{15}N_{18}C_{14}C_{11}$ is assigned at 663, 642 $cm^{-1}$ in FT-IR spectrum, 634 $cm^{-1}$ in FT-Raman spectrum and for the same mode the corresponding harmonic values are 675, 656 $cm^{-1}$ (mode nos: 67, 68).

#### 4.2.7. Methyl group Vibrations

The compound ECM3CTC contains one $CH_2Cl$ group attached to pyrimidine ring. In $CH_2Cl$, the C-H stretching occurs at lesser frequencies than those of aromatic C-H stretching (3100-3000 $cm^{-1}$). The region around 2980 $cm^{-1}$ is assigned to asymmetric C-H stretching mode of $CH_2Cl$ group **[Coluthup et al., 1990, Kleiman, 1977, Smith, 1999 and Socrates 1990]** and the region around 2870 $cm^{-1}$ is allotted to symmetric C-H stretching mode. In asymmetric stretching of $CH_3$ mode, the two C-H bonds of the methyl group are expanding while the third one is contracting. In symmetric stretching of $CH_3$ mode, all the three C-H bonds expand and contract in-phase. The asymmetric stretching for the $CH_3$ has higher magnitude than the symmetric stretching **[Sudha et al., 2011, Varsanyi, 1969 and Socrates, 1980].** In ECM3CTC, the $C_{20}\text{-}H_{21}$and $C_{20}\text{-}H_{22}$ of symmetric and asymmetric stretching vibrations of methyl group did not occur in both FT-IR and FT-Raman region. The expected theoretically values obtained by B3LYP/6-311++G(d,p) method at 3212, 3128 $cm^{-1}$ (mode numbers 6, 10). The substitution of chlorine atom to methyl group has affected the C-H vibration to higher value.

### 4.3. NBO Analysis

NBO analysis is used for studying intra molecular bonding interactions, and also a means to investigating charge transfer or conjugative interaction in molecular systems. Of the different

molecular orbitals, some are electron donors and some are acceptors, the energy difference between such bonding and anti-bonding orbitals makes the molecule susceptible for interactions. The bonding, non-bonding and anti-bonding interactions can be quantitatively described by means of the second-order perturbation interaction energy $E^{(2)}$. This energy represents the estimation of the off-diagonal Fock matrix elements and can be deduced from the second-order perturbation as **[James et al., 2006, Na et al., 2005, Liu et al., 2005]**

$$E^{(2)} = \Delta E_{ij} = q_i \frac{F(i,j)^2}{\varepsilon_j - \varepsilon_i} \quad (5)$$

where $q_i$ is the donor orbital occupancy, $\Sigma_i$ and $\Sigma_j$ are diagonal elements (orbital energies) and F(i,j) is the off diagonal NBO Fock matrix elements. The larger energy difference $E^{(2)}$ value, the more intensive is the interaction i.e. more is donating tendency of electron from one orbital and more is the accepting tendency of other orbital, which makes the interaction between them stronger.

**Table 3. The second order perturbation theory analysis of Fock Matrix in NBO basis for ECM3CTC**

| Type | Donor NBO (i) | ED/e | Acceptor NBO (j) | ED/e | [a]E(2) KJ/mol | [b]E(j)-E(i) a.u. | [c]F(i,j) a.u. |
|---|---|---|---|---|---|---|---|
| π -π* | BD (2) C1 - C6 | 1.65963 | BD*(2) C2 - C3 | 0.3737 | 86.86 | 0.27 | 0.067 |
| | | | BD*(2) C4 - C5 | 0.32409 | 88.24 | 0.28 | 0.069 |
| π -π* | BD (2) C2 - C3 | 1.68165 | BD*(2) C1 - C6 | 0.34885 | 79.24 | 0.3 | 0.068 |
| | | | BD*(2) C4 - C5 | 0.32409 | 80.25 | 0.3 | 0.067 |
| π -π* | BD (2) C4 - C5 | 1.66847 | BD*(2) C1 - C6 | 0.34885 | 80.33 | 0.29 | 0.066 |
| | | | BD*(2) C2 - C3 | 0.3737 | 87.07 | 0.27 | 0.068 |
| π -σ* | BD (2) C11 - C14 | 1.84552 | BD*(1) C1 - C10 | 0.04684 | 14.27 | 0.67 | 0.044 |
| | | | BD*(2) C11 - C14 | 0.24204 | 14.77 | 0.31 | 0.03 |
| | | | BD*(1) C20 - H21 | 0.01685 | 7.57 | 0.72 | 0.034 |
| | | | BD*(2) C24 - O25 | 0.30813 | 98.87 | 0.29 | 0.077 |
| π -π* | BD (2) C12 - O17 | 1.98716 | BD*(2) C12 - O17 | 0.33555 | 8.45 | 0.46 | 0.03 |
| π -π* | BD (2) C24 - O25 | 1.97955 | BD*(2) C11 - C14 | 0.24204 | 20.71 | 0.4 | 0.042 |
| n -σ* | LP (1) N16 | 1.74331 | BD*(1) C1 - C10 | 0.04684 | 34.39 | 0.66 | 0.069 |
| | | | BD*(1) C12 - O17 | 0.0377 | 11.51 | 0.83 | 0.045 |
| | | | BD*(2) C12 - O17 | 0.33555 | 190.25 | 0.32 | 0.11 |
| n -σ* | LP (1) O17 | 1.97516 | BD*(1) C12 - N16 | 0.07435 | 11.55 | 1.14 | 0.051 |
| | | | BD*(1) C12 - N18 | 0.0902 | 8.79 | 1.08 | 0.043 |
| n -σ* | LP (2) O17 | 1.84377 | BD*(1) C12 - N16 | 0.07435 | 103.47 | 0.7 | 0.12 |
| | | | BD*(1) C12 - N18 | 0.0902 | 118.24 | 0.64 | 0.123 |
| n -π* | LP (1) N18 | 1.6622 | BD*(2) C11 - C14 | 0.24204 | 180.25 | 0.3 | 0.104 |
| | | | BD*(2) C12 - O17 | 0.33555 | 182.13 | 0.32 | 0.106 |
| n -σ* | LP (2) Cl23 | 1.98362 | BD*(1) C20 - H21 | 0.01685 | 11.67 | 0.77 | 0.041 |
| | | | BD*(1) C20 - H22 | 0.0158 | 8.08 | 0.78 | 0.035 |
| n -σ* | LP (3) Cl23 | 1.96056 | BD*(1) C14 - C20 | 0.03655 | 18.12 | 0.69 | 0.049 |
| | | | BD*(1) H15 - N18 | 0.02652 | 16.19 | 0.78 | 0.049 |
| n -σ* | LP (1) O25 | 1.97441 | BD*(1) C11 - C24 | 0.05791 | 12.55 | 1.14 | 0.053 |
| n -σ* | LP (2) O25 | 1.84879 | BD*(1) C11 - C24 | 0.05791 | 70.96 | 0.71 | 0.101 |
| | | | BD*(1) C24 - O26 | 0.10017 | 138.62 | 0.62 | 0.13 |
| n -σ* | LP (1) O26 | 1.95769 | BD*(1) C20 - Cl23 | 0.01951 | 7.03 | 0.66 | 0.03 |
| | | | BD*(1) C24 - O25 | 0.01801 | 30.54 | 1.16 | 0.083 |
| n -π* | LP (2) O26 | 1.80713 | BD*(2) C24 - O25 | 0.30813 | 190.08 | 0.33 | 0.113 |
| | | | BD*(1) C27 - H28 | 0.01952 | 17.41 | 0.78 | 0.053 |
| | | | BD*(1) C27 - H29 | 0.01943 | 17.15 | 0.78 | 0.053 |
| n -σ* | LP (2) Cl35 | 1.9737 | BD*(1) C2 - C3 | 0.02575 | 15.77 | 0.88 | 0.052 |
| | | | BD*(1) C3 - C4 | 0.02665 | 15.61 | 0.87 | 0.051 |

[a] $E^{(2)}$ means energy of hyper conjugative interaction (stabilization energy).

[b] Energy difference between donor (i) and acceptor(j) nbo orbitals.
[c] F(i,j) is the Fock matrix element between i and j nbo orbitals.

The $E^{(2)}$ energy values and types of the transition are listed in Table 3. The strong intra-molecular hyperconjugative interaction of the σ and π electrons of C-C, C=C, C=N to the anti C-C, C=C, C=N bonds of the ring as well as C=O group leads to stabilization of some part of the ring system in ECM3CTC. The hyperconjugative interactions in this molecular are $\pi(C_4\text{-}C_5)\rightarrow\pi^*(C_1\text{-}C6)$, $\pi(C_1\text{-}C_6)\rightarrow\pi^*(C_2\text{-}C_3)$, $\pi(C_4\text{-}C_5)\rightarrow\pi^*(C_2\text{-}C_3)$, $\pi(C_1\text{-}C_6)\rightarrow\pi^*(C_4\text{-}C_5)$, $\pi(C_{11}\text{-}C_{14})\rightarrow\sigma^*(C_{24}\text{-}O_{25})$ with corresponding stabilization energy: 80.33 86.86, 87.07, 88.24 &98.87 KJ/Mol respectively. In ECM3CTC, the lone pair of oxygen, and nitrogen atoms play great role, ie the $O_{17,}O_{25,}N_{18,}O_{26}$& $N_{16}$atoms transfer maximum energy 118.24,138.62, 180.25, 182.13, 190.08 & 190.25 KJ/Mol to ($C_{12}$-$N_{18}$), ($C_{24}$-$O_{26}$), ($C_{11}$-$C_{14}$), ($C_{12}$-$O_{17}$), ($C_{24}$-$O_{25}$) & ($C_{12}$-$O_{17}$) bonds, respectively.

In hetero cyclic atoms, the maximum hyperconjugative $E^{(2)}$ energy exhibited during the inter-molecular interaction, which leads the molecule towards medicinal and biological application. According to the stabilization energy values, the first five most probable electronic transitions in this molecule in the descending order are: 1. C2 - C3 to C4 - C5 (π*-π* and $E^2$ = 249.13), 2. C2 - C3 to C4 - C5 (π*-π* and $E^2$ = 238.8), 3. LP(1)N16 to C12 - O17 (n -π*, $E^2$ = 45.47), 4. LP(1)N18 to C12 - O17 (n -π*, $E^2$ = 43.53), and 5. LP(1)N18 to C12 - O17 (n -π*, $E^2$ = 43.08). But among the five most probable transitions, only one or two will take place with high intensity which can be observed in the experimental UV- Visible spectrum also, whose values are determined by the high oscillator strength value.

### 4.4. Molecular docking

Molecular docking studies were carried out to study the precise binding site of ligand on protein. A molecular docking study is a key tool in structural molecular biology and computer-assisted drug design. Molecular docking trials for compound ECM3CTCwas performed by using Glide module implemented in Maestro version 9.3.5 of Schrödinger software suite, 2011. The 3D co-ordinates of crystallographic structure of the Dengue virus NS2B/NS3 protease was retrieved from the Protein Data Bank (PDB) using PDB ID: 3LD6. The Ketoconazole protein (PDB ID: 3LD6) was downloaded from protein Data Bank (http://www.rcsb.org/pdb). The molecular docking studies of the ligands and the protein were performed by GLIDE. Glide provides three different levels of docking precision, high throughput virtual screening (HTVS), standard precision (SP), extra precision (XP). Calculations were carried out in XP mode.

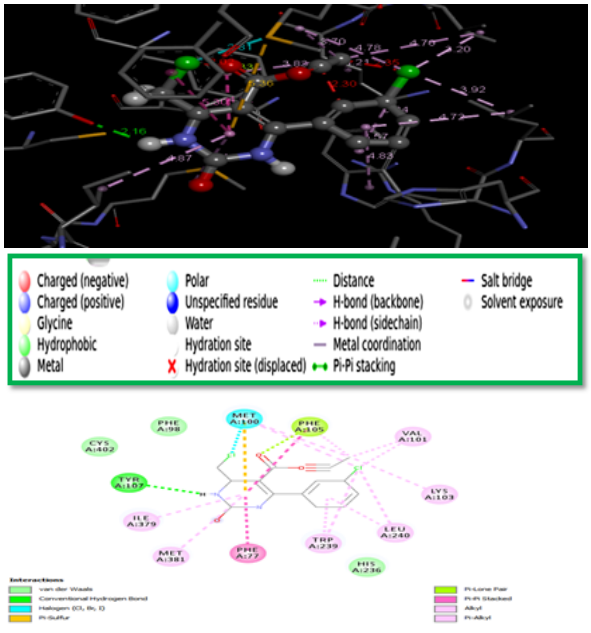


**Fig. 4. 2D and 3D interactions of ECM3CTC**

For the given structures of a ligand and a protein, docking problem is to predict the structures of the resulting complex. The geometry of the complex reflects the global minimum energy **[Chamberlain, 1974]**. The synthesized analogue docked with crystal structure of human lanosterol 14-alpha dimethylase in complex with ketaconazole (3LD6). Analogue showed best ligand pose energy 13.5 kcal/mol in3LD6 protein. The possible number of protein ligand interactions were predicted and shown in Fig.4. The ligand is surrounded by hydrophilic interactions with the amino acids like PHE 104, TYR107, ILE379, MET100, LEU240, MET381, PHE77, VAL101, PHE105 and TRP 239.The TYR107 amino acid interacts with pyrimidine ring and PHE 105 interacts with carboxylate group via hydrogen bonding interaction.The Vander walls interaction within PHEA:98, CYSA:402 and HISA:236 are surrounding the interaction. The protein-ligand interaction value indicates that the synthesized compound ECM3CTC exhibits better anti-inflammatory property. From this interaction it can be predicted as the activity may be due to inhibition of human lanosterol 14-alpha dimethylase in complex with ketaconazole.

### 4.5. UV-Analysis

The UV-Vis absorption spectrum of ECM3CTCis recorded in the range 200-800 nm. The UV-Vis spectral analyses of the molecule have been investigated in Gas phase, Chloroform and DMSO by TD-SCF/B3LYP/6-311++G(d,p) calculations. The electronic transitions, the corresponding excitation energies and the oscillator strengths for the three phases are presented Table 4. From the table, it is found that the electronic transition ofECM3CTC with high oscillator strengths and low absorption wavelength for all the three phases, thereby giving rise to significant electronic properties. The observed and simulated UV–Vis spectra are shown in Fig. 5. Typically, according to the Frank-Condon principle, the maximum absorption peak ($\lambda_{max}$) in a UV-Vis spectrum corresponds to vertical excitation.

The theoretical calculation predicts one intense electronic transition at 303 nm with an oscillator strength f = 0.1233 is in agreement with the experimental data $\lambda_{exp}$ = 300 nm. Since the absorption wavelength lies in the n -π* transition, according to NBO analysis, the following transitions causes the UV-Visible transition. I) LP( 1)N 16 to C 12 - O 17 (n -π*, $E^2$ = 45.47), II) LP( 1)N 18 to C 12 - O 17 (n -π*, $E^2$ = 43.53), and III) . LP( 1)N 18 to C 12 - O 17 (n -π*, $E^2$ = 43.08).

According to the oscillator strength value, only the second transition in the above list appear in the theoretical spectrum. However, the experimental spectrum shows that there is overlapping of all these most probable transitions as their oscillator strengths are close to each other.

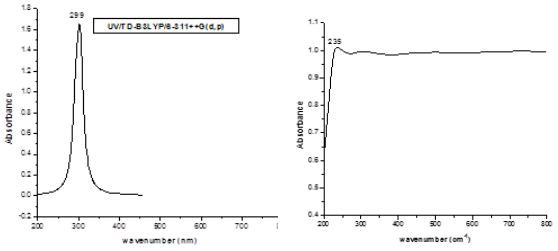


**Fig. 5. The combined calculated and experimental UV Vis spectra of ECM3CTC**

**Table 4. The electronic transition of ECM3CTC using B3LYP/6-311++G(d,p) basis set**

| Calculated at B3LYP/ 6-311++G(d,p) | Oscillator strength | Calculated Band gap (eV/nm) | Experimental Band gap (eV/nm) | Type |
|---|---|---|---|---|
| Excited State-1 | Singlet-A(f=0.0122) | 4.0069eV/309.43nm | | n-π* |
| 83 -> 86 | 0.20686 | | | |
| 84 -> 86 | 0.59833 | | | |
| 85 -> 86 | -0.27667 | | | |
| Excited State-2 | Singlet-A(f=0.1233) | 4.0862eV/303.42nm | | n-π* |
| 82 -> 86 | 0.10804 | | | |
| 83 -> 86 | 0.28378 | | | |
| 84 -> 86 | 0.12259 | | | |
| 85 -> 86 | 0.55827 | | | |
| Excited State-3 | Singlet-A(f=0.0674) | 4.2228 eV/293.61nm | 235 | π-π* |
| 80 -> 86 | 0.17095 | | | |
| 81 -> 86 | 0.12911 | | | |
| 83 -> 86 | 0.5481 | | | |
| 84 -> 86 | -0.2977 | | | |
| 85 -> 86 | -0.17863 | | | |

### 4.6. NMR Spectra Analysis

NMR chemical shift analysis is used to elucidate the types of functional groups in the molecules or samples. It is also used to predict details about the composition and chemical environment of atoms in the molecule. The chemical shifts were computed for H and C atoms in the molecule using B3LYP functional and 6-311++G(d,p) basis set along with GIAO functional, which is meant for this purpose. The same was also experimentally measured using $H^1$ and $C^{13}$ NMR spectrometer and the results were presented in Table 5. The $^1H$ and $^{13}C$ experimental shifts in ppm for the molecule ECM3CTC are also given in Figs. 6a & 6b. The chemical shift for carbon atoms in benzene ring is expected in the range 100-120 ppm, this is found to be the case in this molecule also except for C1whose value is found to be 130 ppm. This observation is in accordance with the charge prediction by MEP where all carbon atoms within benzene are equally negative except C1. Because of the positive charge on C1 the deshielding is more on this atom compared to other atoms which lead to higher chemical shift. The same trend is also observed in Pyrimidine ring, where all positively charged C atoms C12 & C14 are found to have higher chemical shift

due to increased deshielding. The other two carbon atoms C10 & C11 due to the enhanced negative charges show much shielding effect, hence their chemical shift is proportionately less 47.31& 89.93 ppm respectively. Hence, the chemical shift values clearly distinguishes benzene ring and pyrimidine ring and demonstrates that these two rings have different types of conjugations. The carbon atoms in the carboxylate groups have chemical shift values clearly less than 50 ppm which indicate they are aliphatic. The C atom which is attached with the chlorine atom shows the least value around 5 ppm, this indicates the complete change in the environment of this atom.

The chemical shift for all $^{1}$H atoms of ECM3CTC fall in the range of 1.25 – 8.08 ppm. The $^{1}$H chemical shift values of aromatic $^{1}$H atoms have the range 7– 8 ppm. The H atoms in the pyrimidine ring show the values in the range 4 to 6 ppm while in the aliphatic chain around 1 ppm. Thus there is clear distinction in the values of H atoms chemical shifts showing the different types of electronic distribution, even though this is not explicitly visible in charge analysis or in vibrational analysis. The observed $^{1}$H and $^{13}$C NMR spectra of ECM3CTC is plotted in Figs. 6a & 6b.

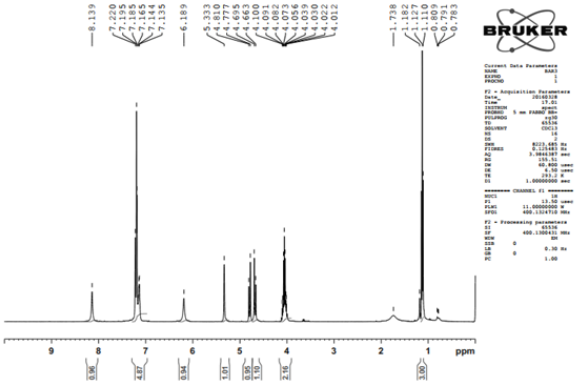


**Fig. 6a. The 1H NMR spectrum of ECM3CTC**

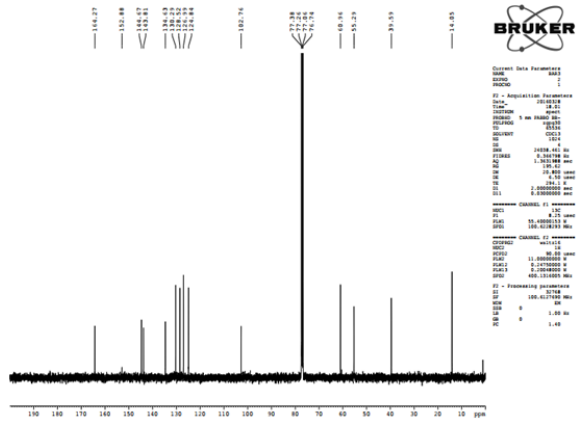


**Fig. 6b. The 13C-NMR spectrum of ECM3CTC**

**Table 5. Theoretical and experimental $^{1}$H and $^{13}$C chemical shift (ppm) of ECM3CTC**

| Atoms | Isotropic chemical shielding tensor (σ) (ppm) | Shift (ppm) | Experimental values Ppm |
|---|---|---|---|
| C1 | 50.96 | 131.5 | |
| C2 | 68.86 | 113.59 | |
| C3 | 52.33 | 130.13 | |
| C4 | 69.13 | 113.33 | |
| C5 | 67.87 | 114.58 | |
| C6 | 74.53 | 107.90 | 102.76 |
| C10 | 135.15 | 47.31 | |
| C11 | 92.33 | 89.93 | |
| C12 | 48.64 | 133.81 | 134.63 |
| C14 | 52.68 | 129.78 | 130.29 |
| C20 | 141.13 | 41.33 | |
| C24 | 32.66 | 149.93 | 152.88 |
| C27 | 129.93 | 52.55 | 55.29 |
| C30 | 177.22 | 5.771 | |
| 7H | 23.79 | 8.08 | 8.139 |
| 8H | 24.43 | 7.44 | |
| 9H | 24.55 | 7.32 | 7.220 |
| 13H | 27.82 | 4.06 | |
| 15H | 25.16 | 6.71 | 6.189 |
| 19H | 26.28 | 5.57 | 5.333 |
| 21H | 27.31 | 4.56 | |
| 22H | 26.98 | 4.90 | 4.810 |
| 28H | 27.52 | 4.35 | |
| 29H | 27.55 | 4.32 | |
| 31H | 30.62 | 1.25 | 1.182 |
| 32H | 30.44 | 1.43 | |
| 33H | 30.42 | 1.45 | |
| 34H | 24.61 | 7.27 | |

## 5. CONCLUSION

The title molecule was synthesized and characterized by spectral analysis such as FTIR, FT-Raman, UV-Vis and NMR spectral studies. A complete vibrational analysis was carried out for the first time for the molecule ECM3CTC. The bond parameters were calculated and also compared with the reported XRD data. NBO analysis reflects the charge transfer occur within the molecule. The Lewis and non-Lewis structure of ECM3CTC provides ED contribution of individual atoms, which leads the molecular vibration with respect to hybridization of chemical bonds. The conjugation of pyrimidine ring π-orbital with carboxylate group σ*-orbital was found to be strong when both orbitals lie in the same plane. Molecular docking studies revealed that the target molecule ECM3CTC exhibited appreciable interaction with 3LD6 protein and the protein-ligand interaction value indicates that the title compound exhibits better anti-inflammatory property. The observed UV-Vis absorption bands are assigned to n-π* & π-π* transition. The chemical shift for all 1H atoms of ECM3CTC fall in the range of 1.25 – 8.08 ppm. The carbon atoms in the carboxylate groups have chemical shift values clearly less than 50 ppm which indicate they are aliphatic. The C atom which is attached with the chlorine atom shows the least value around 5ppm, this indicates the complete change in the environment of this atom. There is clear distinction in the values of H atoms chemical shifts showing the different types of electronic distribution, and therefore confirm the formation of target compound.

## REFERENCES


1. Alam, M., and Lee, D. U. (2016), 64, 185-201.
2. Amir M, Javed SA and Kumar H; Indian J. Pharm. Sciences, 2007; 69(3): 337-343.
3. Amr EA, Nermien MS, Abdulla MM. Monatsh Chem, 2007; 138: 699- 707.
4. Bharanidharan, S., Saleem, H., Gunasekaran, B., Syed Ali Padusha, M., Suresh, M. Crystal structure of ethyl 6-(chloromethyl)-4-(4-chlorophenyl)-2-oxo-1,2,3,4-tetrahydropyrimidine-5-carboxylate, Acta Cryst. 2014, E70, 1185–1186.
5. Beena, K.P., Akelesh, T. Int. Res. J. Pharm. 2012, 3, 303–304.
6. Bist, H.D., Brand, J.C.D., Williams, D.R. J. Mol. Spectrosc. 1967, 24, 402–412.
7. Chamberlain, N. F. The Practice of NMR Spectroscopy with Spectra-Structure Correlations
8. for Hydrogen-1, Plenum Press (1974).
9. Coluthup, N.B., Paly, L.H., Wiberley, S.E. Introduction to Infrared and Raman Spectroscopy, third ed., Academic press, Boston, MA, 1990.
10. Dhandapani, A., Manivarman, S., Subashchandrabose, S., Chem. Phys. Lett. (2016), http://dx.doi.org/10.1016/j.cplett.2016.04.009.
11. Desai K, Patel R, Chikhalia K. J Ind Chem, 2006; 45: 773-778.
12. Evans, J.C. Spectrochim. Acta.1960, 16, 1382–1392.
13. Frisch, M.J., Pople, J.A. Gaussian 03, Revision C.02, Gaussian Inc., Wallingford, CT, 2004.
14. Fujiwara N, Nakajima T, Ueda Y, Fujita HK, Awakami H. Bioorg Med Chem, 2008; 16: 9804-9816
15. Geskin, V.M., Lambert, C.J., Bredas, L. Origin of high second and third-order nonlinear optical response in ammonio/borato diphenylpolyene zwitterions: the remarkable role of polarized aromatic groups, J. Am. Chem. Soc. 125 (2003) 15651-15658.
16. James, C., AmalRaj, A., Reghunathan, R., Hubert Joe, I., JayaKumar, V.S., J. Raman Spectrosc. 37 (2006) 1381–1392.
17. Jamroz, M.H. Vibrational Energy Distribution Analysis: VEDA4 program, Warsaw, Poland, 2004.
18. Khalaji, A. D.,Chermahini, A. N., Fejfarova, K. & Dusek, M. Journal of the Structural
19. Chemistry, (2009) 21,153-157.
20. Kleiman, D.A., phys. Rev. 126 (1962) 1977.
21. Kleinman, D.A., (1962). Nonlinear Dielectric Polarization in Optical Media, Physics Reviews, 126, 1977-1979.
22. Liu, J., Chen, Z., and Yuan, S. Journal of Zhejiang University Science, 6B(6),(2005), 584-589.
23. Meganathan, C., Sebastian, S., Kurt, M., Lee, K. W., & Sundaraganesan, N. Journal of
24. Raman Spectroscopy, 41(10), (2010), 1369-1378.
25. Michalska, D. Raint Program, Wroclaw University of Technology, 2003.
26. Michalska, D. and Wysokinski, R. Chem. Phys. Lett., 403 (2005) 211-217.
27. Mooney, M.F., Spectrochim. Acta 20 (1964) 1021.
28. Mooney, E.F., Spectrochim. Acta 19 (1963) 877.
29. Na, L.J., Rang, C.Z., Fang, Y.S., Zhejiang, J., Univ. Sci. 6B (2005) 584–589.
- Stanisaw, Jord. J. Chem, (2009), 4: 1-15.
30. Radom, L., John A. Pople, J. American. Chem. Soc. 92 (1970) 4786-4795
31. Roeges, N.P.G. A Guide to the Complete Interpretation of Infrared Spectra of Organic Compounds, Wiley, New York, 1994.

32. Sarojini, K., Krishnan, H., Charles Kanakam, C., Muthu, S., Spectrochim. Acta A108 (2013) 159-170
33. Schlegel, H.B. J. Comput. Chem. 1982, 3, 214–218.
34. Sharma, A.; Khare, R.; Kumar, V.; Gupta, G. K.; Beniwal, V. Int. J. Pharm. Pharm.
35. Sci.2014, 6, 171–175.
36. Sasada, T., Kobayashi, F., Sakai, N., Konakahara, T., Organic Letters, 2009; 11: 2161-2164.
37. Scott, A.P., Random, L., J. Phys. Chem. 100 (1996) 16502-16513.
38. Silverstein, R.M., and Webstor, F.X. Spectrometric identification of organic compounds
39. sixth edn. Wiley, New York(1998).
40. Smith, B., Infrared Spectral Interpretation. A Systematic Approach, CRC Press, Washington,
41. D C, 1999.
42. Socrates, G. Infrared Characteristics Frequencies, Wiley-interscience Publication, New York, 1990.
43. Socrates, G. Infraredand Raman Characteristic group Frequencies, Tables and Charts, 3rd
44. Ed. Wiley, Chichester(2001).
45. Sudha, S. Karabacak, M. Kurt, M. Cinar, M. Sundraganesan, N. Spectrochim. Acta A 84 (2011) 184-195.
46. Sundaraganesan, N., Meganathan, C., Joshua, B.D., Mani, P., Jayaprakash, A.,
47. Spectrochim. Acta A 71 (2008) 1134-1139.
48. Vaisalini, N.B., Rao, N.V., Harika, V.B.M.L., Desu, P.K., Nama, S., .Int. J. Pharm. Chem.
49. Res. 2012,
50. Varghese, H. T., Panicker, C. Y., Madhavan, V. S., Mathew, S., Vinsova, J., & Van.
51. Alsenoy, C. Journal of Raman Spectroscopy, 40(9),(2009), 1211-1223
52. Varsanyi, G., Assignments for Vibrational Spectra of Seven Hundre Benzene Derivatives,
53. vol. 1/2, Academic Kiado, Budagset, (1973), 2278–8700.
54. Varsanyi, G. Vibrational Spectra of Benzene Derivatives, Academic Press, New York, 1969.
55. Wagner E, Al-Kadasi K, Zimecki M, Sawka-Dobrowolska W. Eur J Med Chem, 2008; 43: 2498-2504.